Electronic Supplementary Material (ESI) for Journal of Materials Chemistry A.

Supporting Information

A synthetic strategy towards single crystal of Zr_6 cluster and phosphonate based metal–organic framework

Haomiao Xie, [a] Kent O. Kirlikovali, [a] Zhijie Chen, [a] Karam B. Idrees, [a] Timur Islamoglu, [a] and Omar K. Farha *, [a, b]

[a] Department of Chemistry, Northwestern University, Evanston, Illinois 60208, United States.

[b] Department of Chemical and Biological Engineering, Northwestern University, 2145 Sheridan Road, Evanston, Illinois 60208, United States

Email: o-farha@northwestern.edu

Table of Contents

Part I. Material Preparations and Characterizations

All reagents were purchased from commercial sources and used as received.
The linkers, **H_2BDPi**, **H_2NDPi and H_2BPDPi** were synthesized following a modified published procedure as below.

Synthesis of 1,4-Benzenediphosphinic Acid(H_2BDPi)

A 25 mL microwave tube was charged with 1,4-dibromobenzene(1.51 g, 6.4 mmol) and anilinium hypophosphite (3.0 g, 18.8 mmol), Xantphos(70 mg, 0.12 mmol), Tris(dibenzylideneacetone)dipalladium(0) chloroform adduct ($Pd_2(dba)_3 \cdot CHCl_3$, 50 mg, 0.05 mmol) and purged with N_2. Then 16 mL degased THF was added followed by 4.4 mL triethylamine. The reaction mixture were heated with microwave reactor at 130 ℃ for 35 minutes. After cooling down to room temperature, the solvent was removed by vacuum and the residual was dissolved in 300 mL NaOH (aq, 1 M) solution. The aqueous solution was washed with 100 mL diethyl ether for three times and acidified with concentrated HCl (12 M, 30 mL), stirred at room temperature for 30 minutes and filtered. The solvent of the filtrate was evaporated by rotovap and the white residual was extracted with 400 mL hot acetone/ethanol mixture (1:1, v/v). The solvent was evaporated and 1.1 g (83% yield) white powder product was obtained and used without further purification. ^{1}H-NMR (500 MHz, DMSO-d_6) δ 7.86 (dd, J = 17.6, 6.0 Hz, 4H), 7.52 (P-H, d, $J_{H\text{-}P}$ = 552.9 Hz, 2H). ^{31}P-NMR (202 MHz, DMSO-d_6) δ 15.23 (d, $J_{H\text{-}P}$ = 552.4 Hz). ^{31}P{^{1}H}-NMR (202 MHz, DMSO-d_6) δ 15.23.

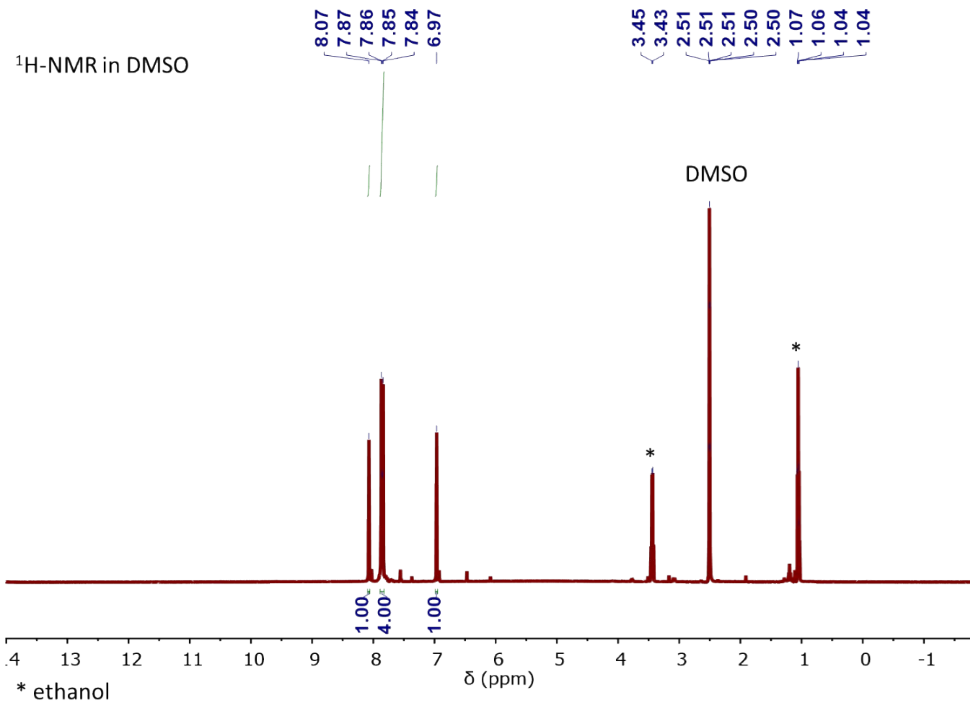

Figure S1. ^{1}H NMR spectrum of H_2BDPi

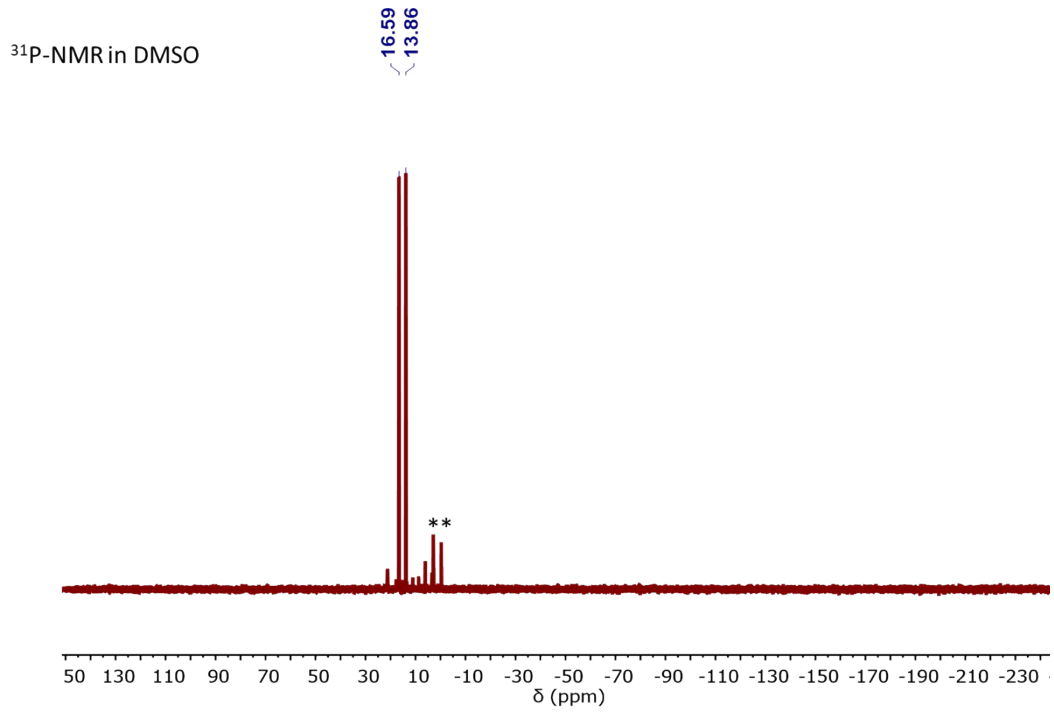

Figure S2. ^{31}P NMR spectrum of H_2BDPi

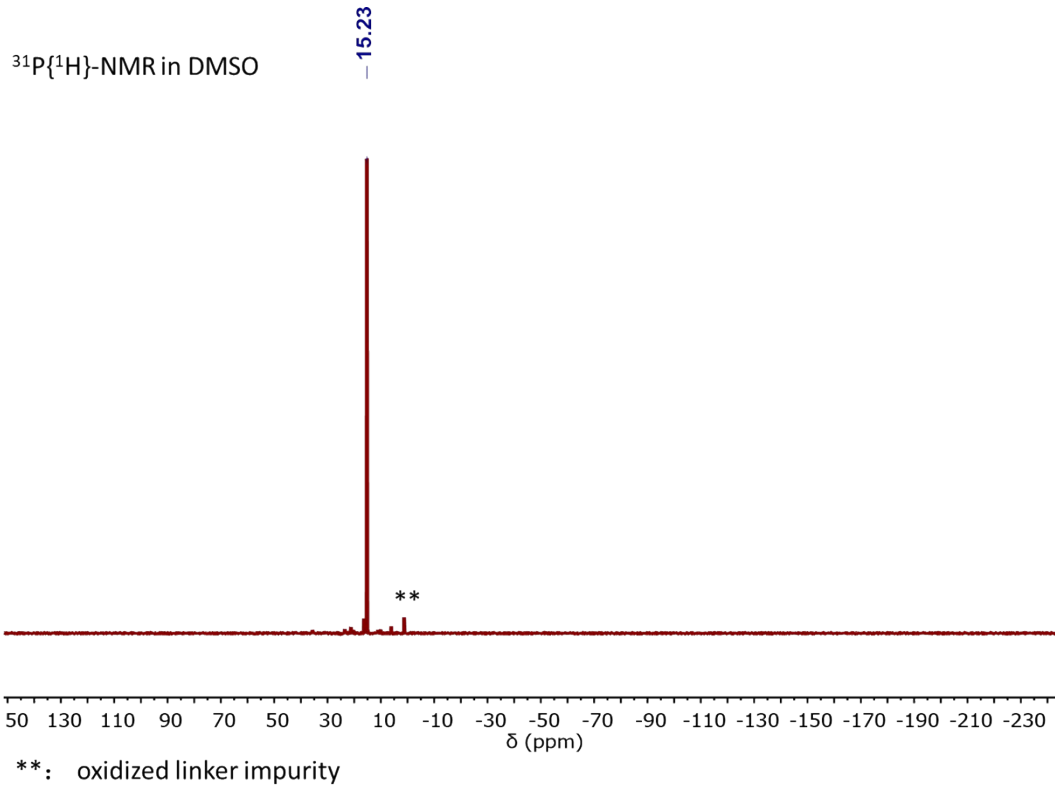

Figure S3. ^{1}H decoupled $^{3}P\{^{1}H\}$ NMR spectrum of H_2BDPi

Synthesis of 2,6-Naphthalenediphosphinic Acid(H_2NDPi)

A 25 mL microwave tube was charged with 2,6-dibromobenzene (0.915 g, 3.2 mmol) and anilinium hypophosphite (1.5 g, 9.4 mmol), Xantphos (35 mg, 0.06 mmol), Tris(dibenzylideneacetone)dipalladium(0) chloroform adduct ($Pd_2(dba)_3 \cdot CHCl_3$, 25 mg, 0.025 mmol) and purged with N_2. Then 16 mL degased THF was added followed by 2.2 mL triethylamine. The reaction mixture were heated with microwave reactor at 120 ℃ for 20 minutes. After cooling down to room

temperature, the solvent was removed by vacuum and the residual was dissolved in 150 mL NaOH (aq, 1 M) solution. The aqueous solution was washed with 50 mL diethyl ether for three times. The solution was then acidified to pH = 7 and filtered again. Additional concentrated HCl (12 M, 15 mL) was added. The formed precipitate was filtered, washed with water and acetone and dried in air. 0.53 g (65% yield) white powder was obtained and used without further purification. ^{1}H-NMR (500 MHz, DMSO-d_6) 8.43 (dd, J = 15.5, 1.2 Hz, 2H), 8.26 (dd, J = 8.4, 2.9 Hz, 2H), 7.84 (ddd, J = 11.3, 8.3, 1.4 Hz, 2H).

7.64 (P-H, d, $J_{H\text{-}P}$ = 551.7 Hz, 2H). ^{31}P-NMR (202 MHz, DMSO-d_6) δ 16.03 (d, $J_{H\text{-}P}$ = 552.0 Hz, 13.5 Hz) ^{31}P{^{1}H}-NMR (202 MHz, DMSO-d_6) δ 16.03.

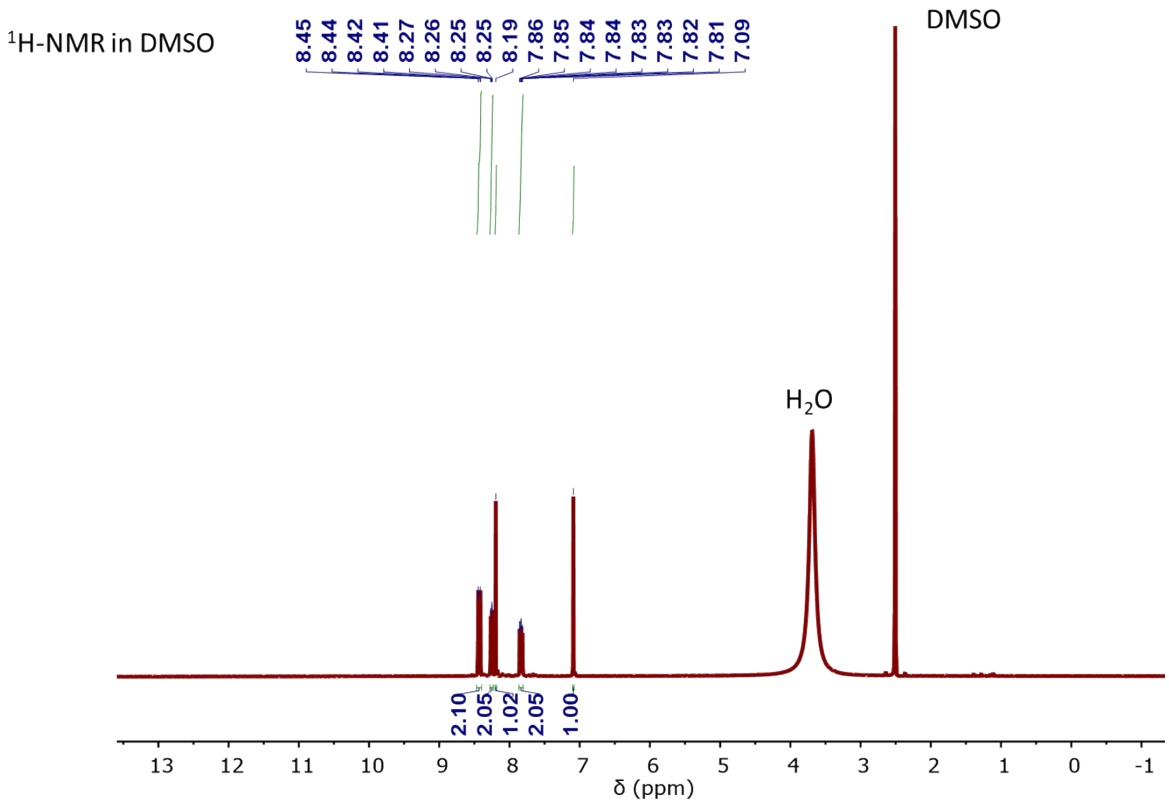

Figure S4. ^{1}H NMR spectrum of H_2NDPi

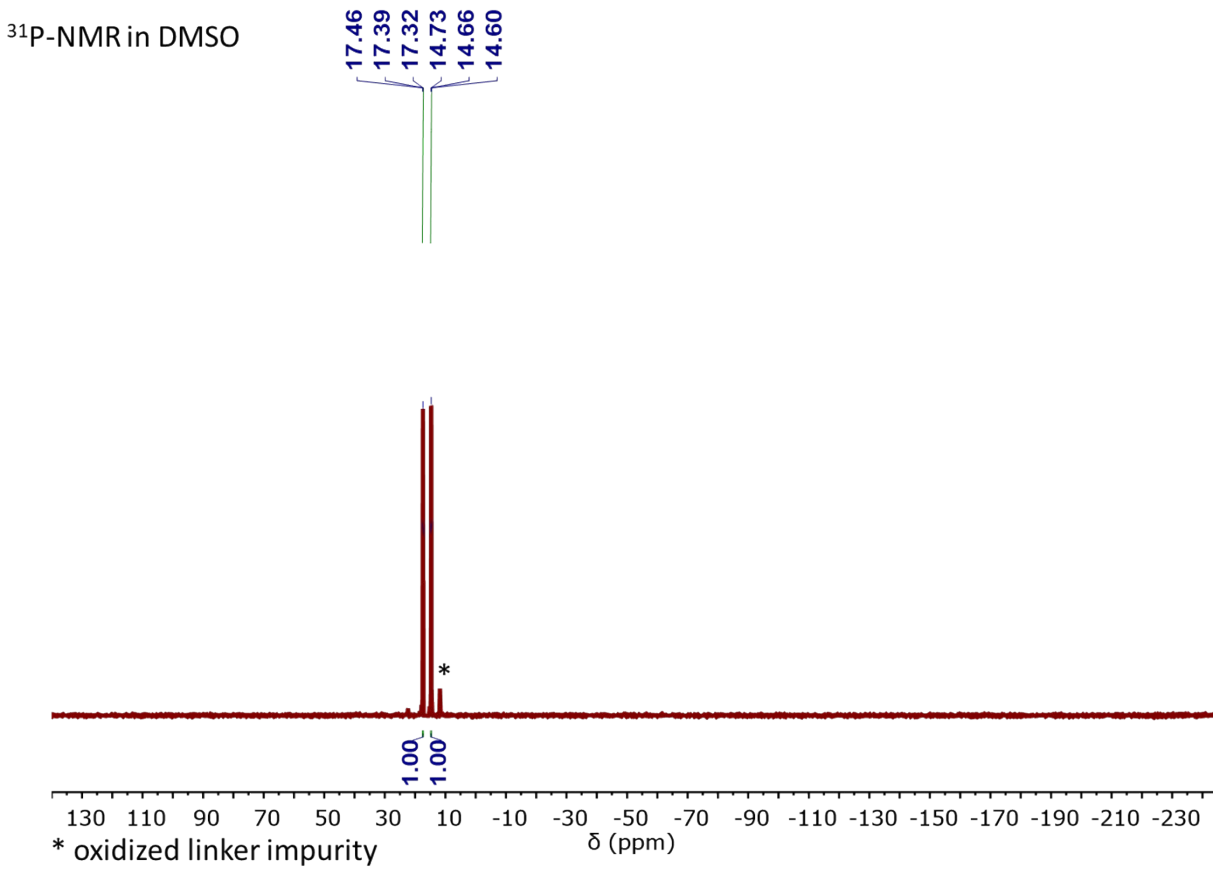

Figure S5. ^{31}P NMR spectrum of H_2NDPi

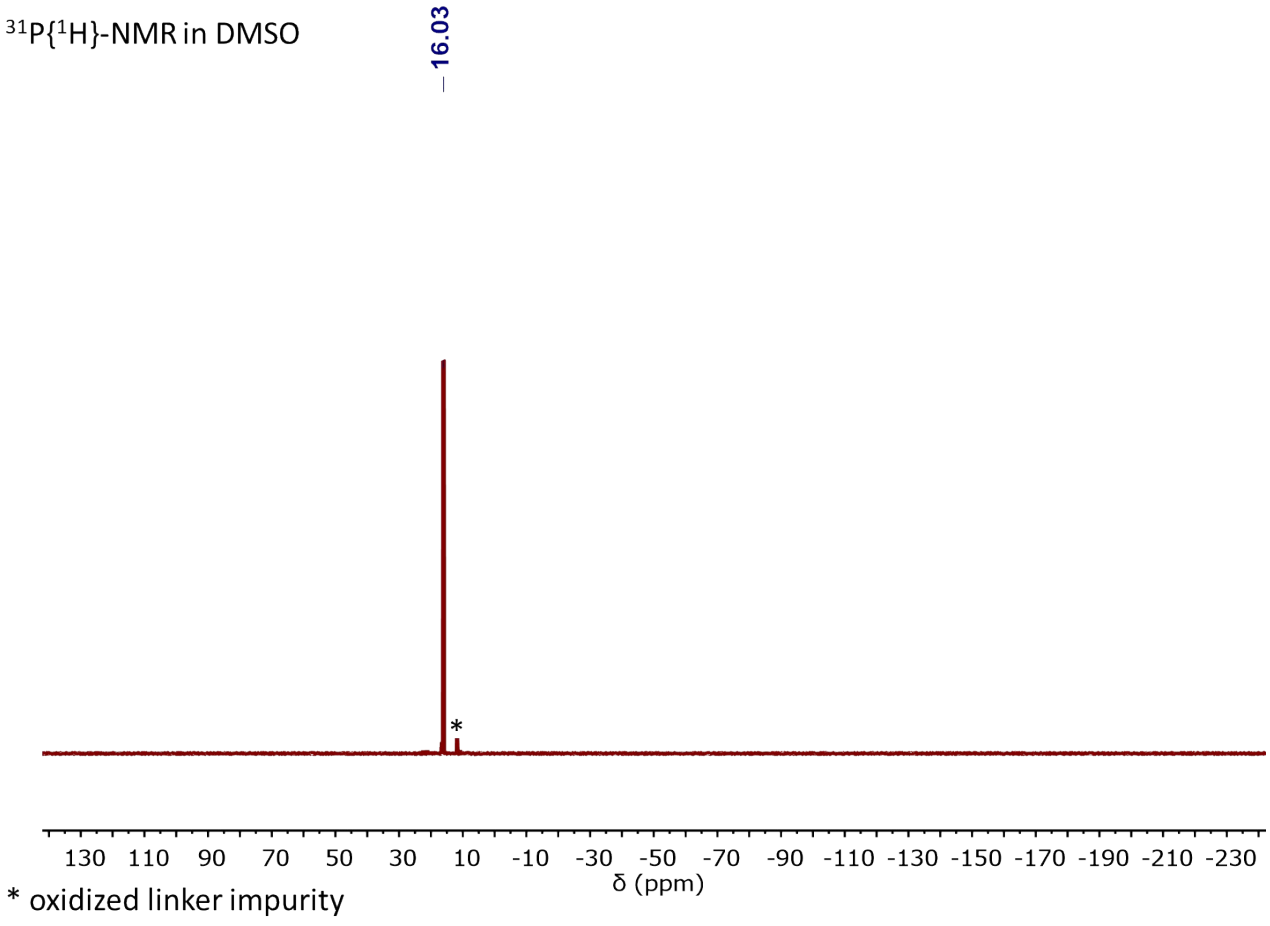

Figure S6. $^{31}P\{^1H\}$ NMR spectrum of H_2NDPi

Synthesis of biphenyl-4,4'-diphosphinic Acid(H_2BPDPi)

A 25 mL microwave tube was charged with 4.4'-dibromobiphenyl(0.80 g, 2.5 mmol) and anilinium hypophosphite (1.2 g, 7.5 mmol), Xantphos (23 mg, 0.04 mmol), Tris(dibenzylideneacetone)dipalladium(0) chloroform adduct ($Pd_2(dba)_3 \cdot CHCl_3$, 20 mg, 0.02 mmol) and purged with N_2. Then 16 mL degased THF was added followed by 2.0 mL triethylamine. The reaction mixture were heated with microwave reactor at 120 ℃ for 10 minutes. After cooling down to room temperature, the solvent was removed by vacuum and the residual was dissolved in 120 mL NaOH (aq, 1 M) solution. The aqueous solution was washed with 50 mL diethyl ether for three times. The solution was then acidified to pH = 7 and filtered again. Additional concentrated HCl (12 M, 12 mL) was added. The formed precipitate was filtered, washed with water and acetone and dried in air. 0.62 g (89% yield) white powder was obtained and used without further purification. ^{1}H-NMR (500 MHz, DMSO-d_6) 7.90 (dd, J = 8.3, 2.7 Hz, 4H), 7.82 (dd, J = 13.1, 8.3 Hz, 4H), 7.54 (P-H, d, J_{H-P} = 549.5 Hz, 2H). ^{31}P-NMR (202 MHz, DMSO-d_6) δ 15.92 (d, J_{H-P} = 549.7 Hz, 13.3 Hz) ^{31}P{^{1}H}-NMR (202 MHz, DMSO-d_6) δ 15.92.

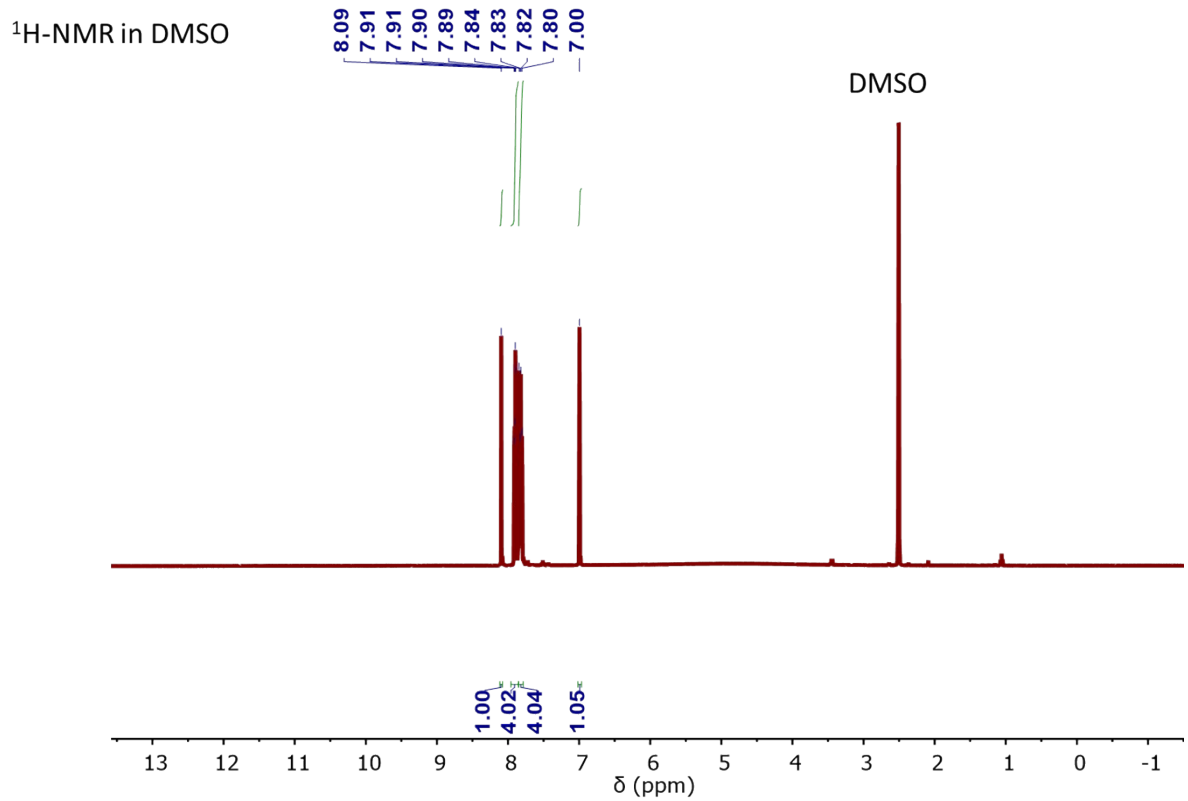

Figure S7. ^{1}H NMR spectrum of H_2BPDPi

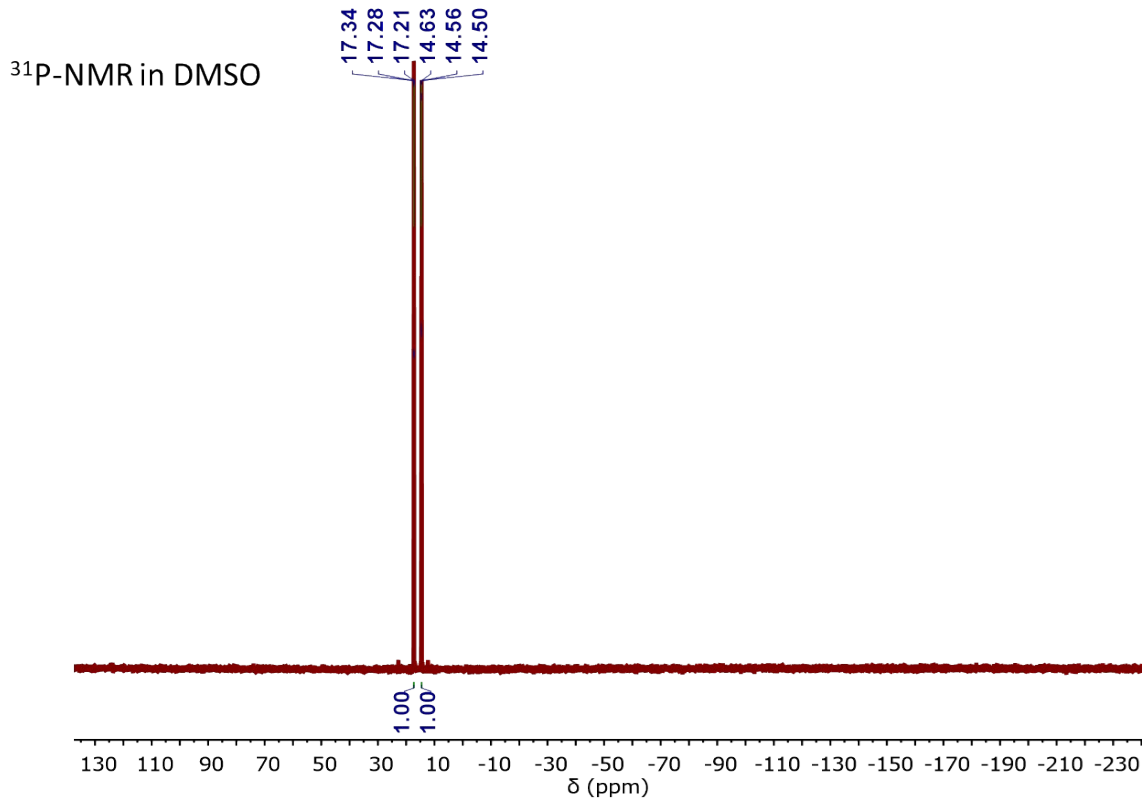

Figure S8. ^{31}P NMR spectrum of H_2BPDPi

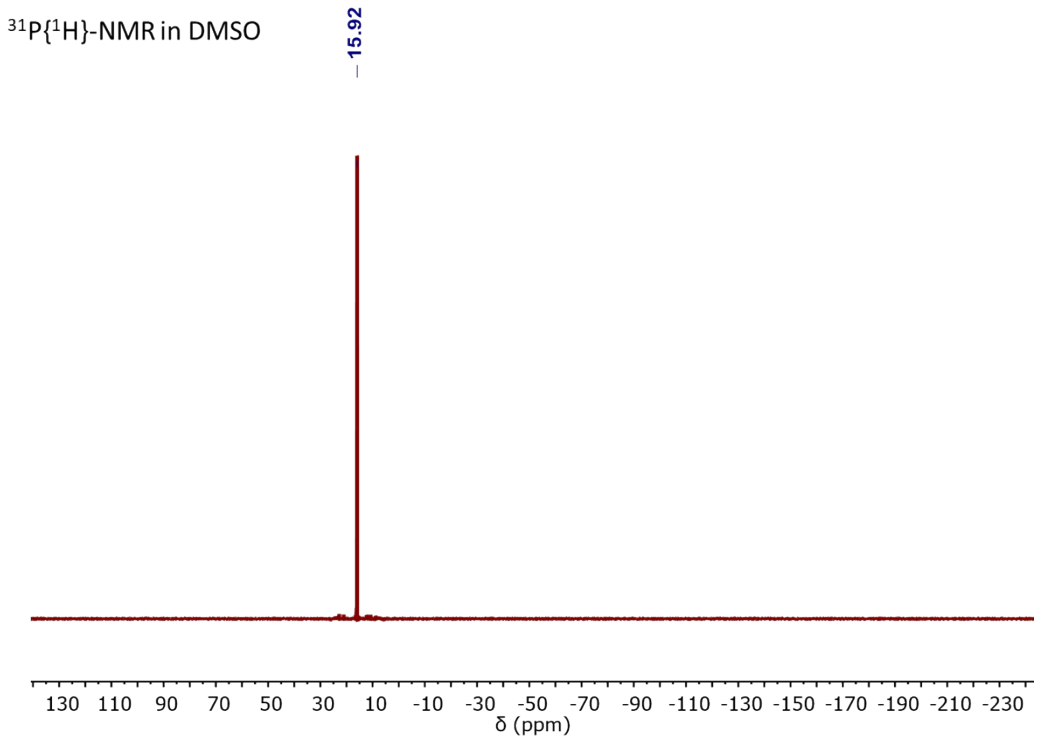

Figure S9. $^{31}P\{^1H\}$ NMR spectrum of H_2BPDPi

Synthesis of parent MOFs: UiO-66, UiO-67 and DUT-52(DUT-52)

The powder samples and single-crystal samples of the parent MOFs, UiO-66, UiO-67 and DUT-52 were synthesized by procedures reported in the literature.[1, 2]

Synthesis of NU-406 via solvent-assisted ligand exchange (SALE)

A 2-dram vial was charged 20 mg (10 μmol) DUT-52 crystalline powder sample, 50 mg (0.19 mmol, 3.2 eq) NDPi and 4 mL DMF with 30 μL TFA. The vial was kept in a 100 ℃ oven for 2 hours. After the 2-hour incubation, the solution phase was removed while hot and washed with fresh DMF for 3 times and then followed with solvent exchange with MeCN. The single-crystal sample was prepared under sample condition but with single-crystal DUT-52. The conversion was confirmed by single-crystal X-ray diffraction, PXRD, ^{1}H NMR and ^{31}P NMR. The sample for gas sorption characterizations were activated under 65 ℃ for 3 hours than followed by 85 ℃ for another 12 hours.

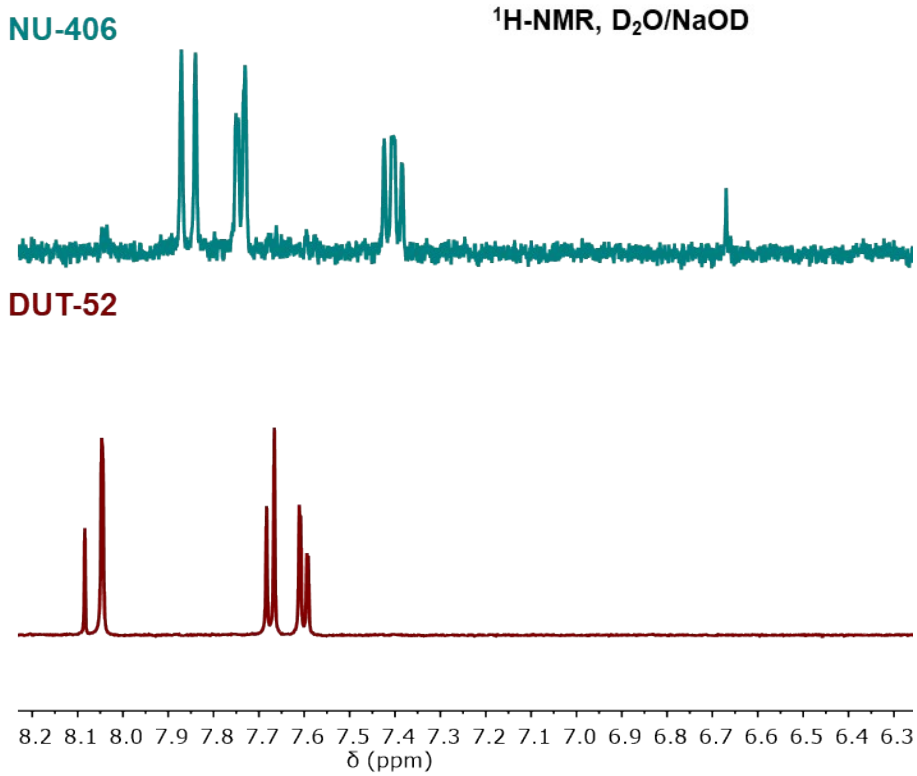

Figure S10. ^{1}H NMR of spectra of DUT-52 and its SALE product NU-406

Synthesis of NU-410 via SALE

A 2-dram vial was charged 20 mg (9.4 μmol) UiO-66 crystalline powder sample, 50 mg (0.18 mmol, 3.1 eq) BPDPi and 4 mL DMF with 30 μL TFA. The vial was kept in a 100 ℃ oven for 24 hours. After the 24-hour incubation, the solution phase was removed while hot and washed with fresh DMF for 3 times and then followed with solvent exchange with MeCN. The single-crystal sample was prepared under sample condition but with single-crystal DUT-52. The conversion was confirmed by single-crystal X-ray diffraction, PXRD, ^{1}H NMR and ^{31}P NMR. The sample for gas sorption characterizations were activated under 65 ℃ for 3 hours than followed by 85 ℃ for another 12 hours.

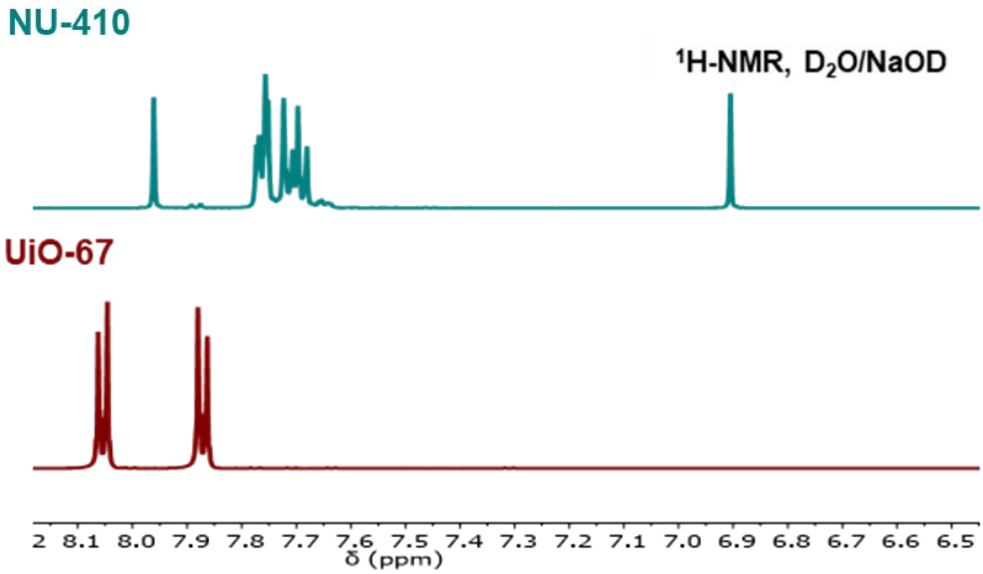

Figure S11. ^{1}H NMR of spectra of UiO-67 and its SALE product NU-410

Synthesis of NU-408 via SALE

A 2-dram vial was charged 15 mg (9.0 μmol) UiO-66 crystalline powder sample, 50 mg (0.24 mmol, 4.5 eq) BDPi and 4 mL DMF with 30 μL TFA. The vial was kept in a 100 ℃ oven for 4 hours. After the 4-hour incubation, the solution phase was removed while hot and washed with fresh DMF for 3 times and then followed with solvent exchange with MeCN. The single-crystal sample was prepared under sample condition but with single-crystal DUT-52. The conversion was confirmed by PXRD, ^{1}H-NMR and ^{31}P-NMR. The sample for gas sorption characterizations were activated under 65 ℃ for 3 hours than followed by 85 ℃ for another 12 hours.

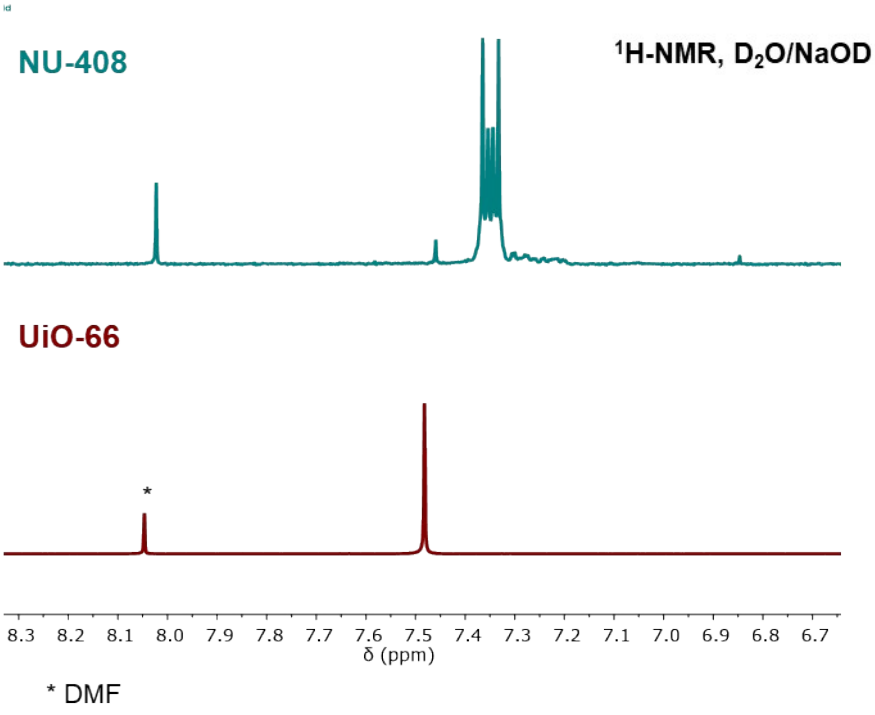

Figure S12. ^{1}H NMR of spectra of UiO-66 and its SALE product NU-408

Post-synthetic oxidation of NU-406 to NU-407

The NU-406 (20 mg, 9.1 μmol) sample was dispersed in 1 mL MeCN solution in a 2-dram vial. t-butyl hydroperoxide(1.0 mL, 6 M in decane) and 0.1 M HCl (aq, 0.4 mL) were added. The reaction mixture was kept in an 80 ℃ oven for 24 hr and then another portion of t-butyl hydroperoxide (1.0 mL, 6 M in decane) was added and incubated at 80 ℃ for another 48 hr. The crystal turns from colorless to pale yellow. After cooling down to room temperature, the solution phase was removed and the solid sample was washed with MeCN for 3 times at 80 ℃. The sample for gas sorption characterizations were activated under 65 ℃ for 3 hours than followed by 85 ℃ for another 12 hours.

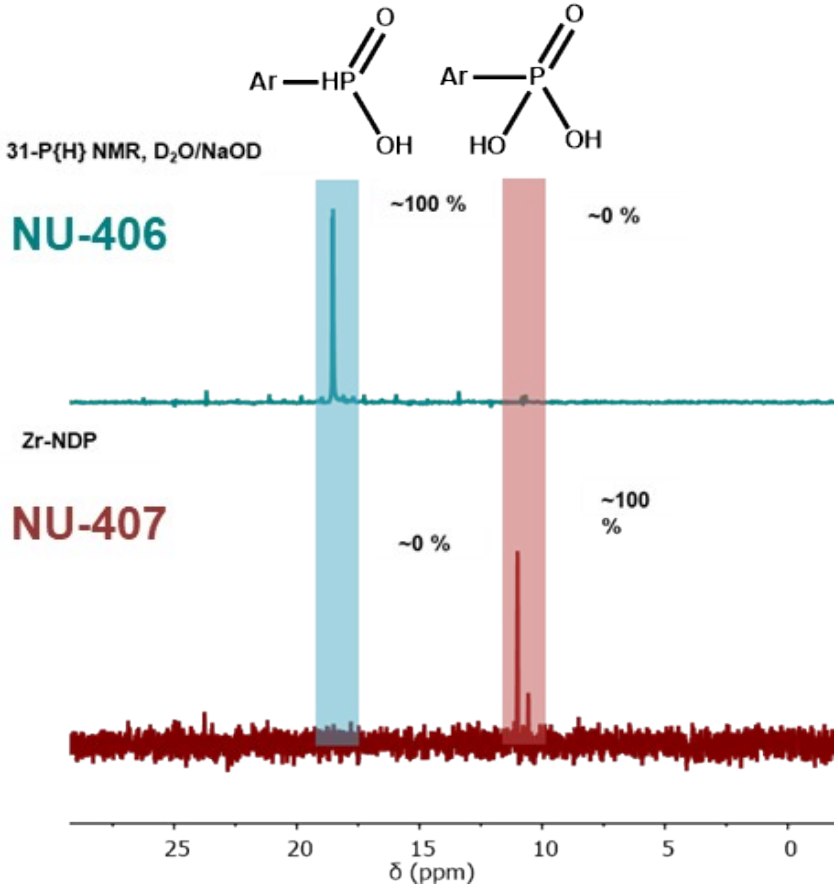

Figure S13. $^{31}P\{^{1}H\}$ NMR spectra of NU-406 and the post-synthetically oxidized product NU-407

Post-synthetic oxidation of NU-408 to NU-409

The NU-406 (20 mg) sample was dispersed in 1 mL MeCN solution in a 2-dram vial. hydrogen peroxide (30 %, 0.3 mL) and 0.1 M HCl (aq, 0.4 mL) were added. The reaction mixture was kept in a 60 ℃ oven for 24 hr and then another portion of hydrogen peroxide hydrogen peroxide (30 %, 0.3 mL)was added and incubated at 60 ℃ for another 72 hr. The crystal turns from colorless to pale yellow. After cooling down to room temperature, the solution phase was removed and the solid sample was washed with MeCN for 3 times at 80 ℃. The sample for gas sorption characterizations were activated under 65 ℃ for 3 hours than followed by 85 ℃ for another 12 hours.

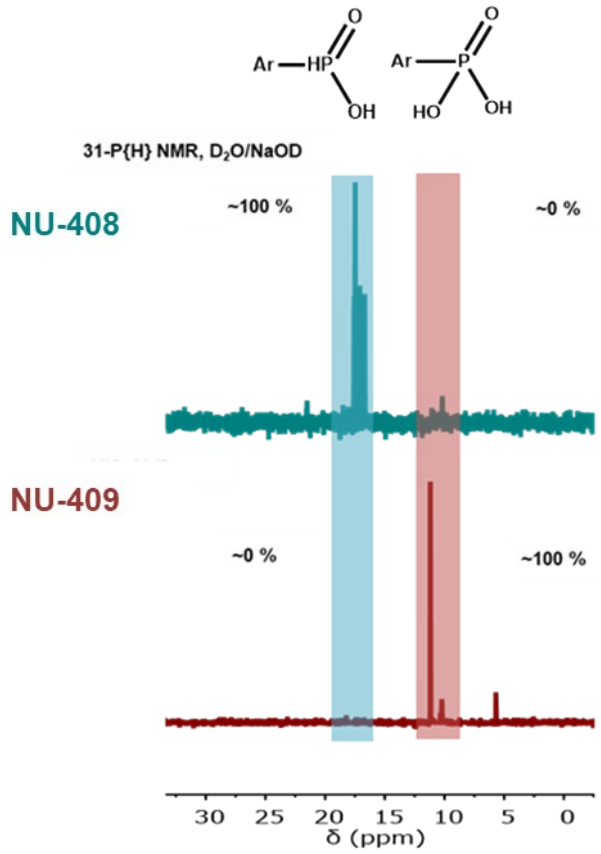

Figure S14. $^{31}P\{^{1}H\}$ NMR spectra of NU-408 and the post-synthetically oxidized product NU-409

Post-synthetic oxidation of NU-410 to NU-411

The NU-410 (20 mg) sample was dispersed in 1 mL MeCN solution in a 2-dram vial. t-butyl hydroperoxide (1.0 mL, 6 M in decane) and 0.1 M HCl (aq, 0.4 mL) were added. The reaction mixture was kept in a 80 ℃ oven for 24 hr and then another portion of t-butyl hydroperoxide (1.0 mL, 6 M in decane) was added and incubated at 80 ℃ for another 48 hr. The crystal turns from colorless to pale yellow. After cooling down to room temperature, the solution phase was removed and the solid sample was washed with MeCN for 3 times at 80 ℃. The sample for gas sorption characterizations were activated under 65 ℃ for 3 hours than followed by 85 ℃ for another 12 hours.

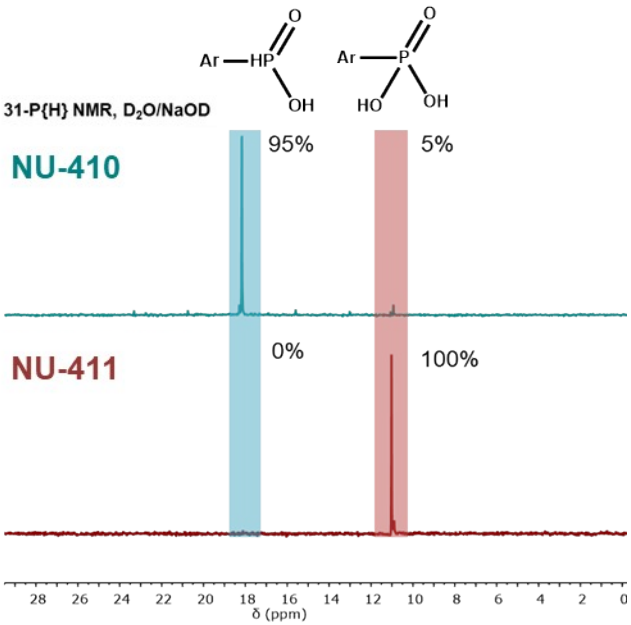

Figure S15. $^{31}P\{^{1}H\}$ NMR spectra of NU-410 and the post-synthetically oxidized product NU-411

Part II. Structural Characterizations

Powder X-ray Diffraction (PXRD) data were measured on a STOE-STADIP powder diffractometer equipped with an asymmetric curved Germanium monochromator (CuKα1 radiation, λ = 1.54056 Å) and one-dimensional silicon strip detector (MYTHEN2 1K from DECTRIS) at 40 kV voltage and 40 mA current in transmission geometry.

Single-Crystal X-ray Diffraction. Single-crystal X-ray diffractions were performed by using a Rigaku Cu-Synergy diffractometer with Cu Kα X-ray radiation (λ = 1.54184 Å) equipped with a shutter-less electronic-noise free Hybrid Photon Counting(HPC) detector and a Cryostream 80-500K (Cryostream Oxford Cryosystems, Oxford, United Kingdom). The single crystals were mounted on MicroMesh (MiTeGen) with paratone oil at low temperature under a nitrogen cryostream at 100 K. The structures were determined by intrinsic phasing (SHELXT 2018/2)[1] and refined by full-matrix least-squares refinement on F^1 (SHELXL-2018/3)[2] using the Olex2[3] software package. Refinement results are summarized in Table S1. Crystallographic data in CIF format have been deposited in the Cambridge Crystallographic Data Centre (CCDC) under deposition numbers 2260133-2260135.

Structural and Powder X-ray Diffraction Simulations. The structures of NU-408, NU-409 and NU-411 were simulated by modifying the solved structures of NU-406, ZrNDP and NU-410 based on experimental PXRD patterns. The simulations structures are done under *Pa-3* space group to prevent the disorder and raised to *Fm-3m* space group to simulate the PXRD patterns.

X-ray photoelectron spectroscopy (XPS) measurements were conducted at the KECKII/NUANCE facility at Northwestern University using a Thermo Scientific ESCALAB 250 Xi instrument, which is equipped with both an electron flood gun and a scanning ion gun. The analysis of XPS data was performed using the Thermo Scientific Avantage Data System software. Furthermore, all spectra were calibrated referencing the C1s peak at 284.8 eV.

Table S1. Crystal data and structure refinement for NU-406, NU-407 and NU-410

Identification code	NU-406	NU-407	NU-410
Empirical formula	$C_{60}H_{36}O_{32}P_{12}Zr_6$	$C_{60}H_{36}O_{44}P_{12}Zr_6$	$C_{72}H_{48}O_{32}P_{12}Zr_6$
Formula weight	2187.85	2379.85	2344.06
Temperature/K	100.15	100.15	100.15
Crystal system	cubic	cubic	cubic
Space group	Fm-3m	Fm-3m	Fm-3m
a/Å	24.6280(3)	23.832(2)	27.5175(5)
b/Å	24.6280(3)	23.832(2)	27.5175(5)
c/Å	24.6280(3)	23.832(2)	27.5175(5)
α/°	90	90	90
β/°	90	90	90
γ/°	90	90	90
Volume/Å^3	14937.8(5)	13536(4)	20836.6(11)
Z	4	4	4
ρ_{calc} g/cm^3	0.973	1.168	0.747
μ/mm^{-1}	4.914	5.531	3.544
F(000)	4288	4672	4624
Crystal size/mm^3	0.15 × 0.12 × 0.1	0.15 × 0.12 × 0.1	0.14 × 0.12 × 0.1
Radiation	CuKα (λ = 1.54184)	CuKα (λ = 1.54184)	CuKα (λ = 1.54184)
2Θ range for data collection/°	6.216 to 135.782	10.5 to 72.732	9.09 to 100.762
Index ranges	-14 ≤ h ≤ 26, -20 ≤ k ≤ 29, -23 ≤ l ≤ 27	-6 ≤ h ≤ 16, -15 ≤ k ≤ 18, -18 ≤ l ≤ 12	-21 ≤ h ≤ 27, -17 ≤ k ≤ 27, -21 ≤ l ≤ 24
Reflections collected	3719	1233	4896
Independent reflections	728 [R_{int} = 0.0302, R_{sigma} = 0.0182]	201 [R_{int} = 0.0460, R_{sigma} = 0.0228]	608 [R_{int} = 0.0330, R_{sigma} = 0.0143]
Data/restraints/parameters	728/281/88	201/119/97	608/177/106
Goodness-of-fit on F^2	1.085	1.14	1.139
Final R indexes [I>=2σ (I)]	R_1 = 0.1082, wR_2 = 0.2977	R_1 = 0.1330, wR_2 = 0.3553	R_1 = 0.0991, wR_2 = 0.2412
Final R indexes [all data]	R_1 = 0.1127, wR_2 = 0.3031	R_1 = 0.1440, wR_2 = 0.3865	R_1 = 0.1049, wR_2 = 0.2458
Largest diff. peak/hole / e Å^{-3}	1.34/-1.04	1.32/-0.80	0.54/-0.63
CCDC number	2260133	2260134	2260135

Table S2. Structural parameters of simulated structures of NU-408, NU-409 and NU-411

Identification code	NU-408	NU-409	NU-411
Empirical formula	$C_{36}H_{24}O_{32}P_{12}Zr_6$	$C_{36}H_{24}O_{44}P_{12}Zr_6$	$C_{72}H_{48}O_{44}P_{12}Zr_6$
Formula weight	1887.59	2079.58	2536.15
Crystal system	cubic	cubic	cubic
Space group	Pa-3	Pa-3	Pa-3
a/Å	21.55	20.85	25.43
b/Å	21.55	20.85	25.43
c/Å	21.55	20.85	25.43
α/°	90	90	90
β/°	90	90	90
γ/°	90	90	90
Volume/Å^3	10010	9064	16450
Z	4	4	4
ρ_{calc} g/cm^3	1.253	1.524	1.024

Table S3. Atomic fractional coordinates of simulated NU-408 in an asymmetric unit

Atom	x	y	z
O	0.07757	0.01057	0.16756
C	0.25825	-0.00223	0.19760
H	0.27253	-0.01004	0.15009
O	0.59166	-0.00665	0.66026
C	0.77497	-0.01394	0.67817
H	0.78904	-0.02150	0.63055
C	0.19487	-0.00507	0.21333
P	0.13649	-0.03663	0.15606
C	0.71159	-0.01665	0.69398
P	0.65233	-0.04672	0.63677
O	0.00307	0.07603	0.83224
C	0.00926	0.25700	0.80412
H	0.01322	0.27139	0.85207
O	0.00238	0.59252	0.33851
C	-0.00234	0.77635	0.32092
H	0.00181	0.79057	0.36891
O	0.95059	0.44424	0.43860
Zr	-0.00493	0.00645	0.11226
O	0.44218	0.94218	0.55782

Table S4. Atomic fractional coordinates of simulated NU-409 in an asymmetric unit

Atom	x	y	z
Zr	-0.00628	0.00811	0.11529
O	0.07770	0.01193	0.17361
C	0.25669	-0.00047	0.19828
H	0.27225	-0.00910	0.14949
O	0.59606	-0.01002	0.66332
C	0.77795	-0.01739	0.67351
H	0.79281	-0.02539	0.62437
O	0.00624	0.07589	0.82623
C	0.01445	0.25572	0.80348
H	0.02036	0.27171	0.85255
O	0.00315	0.59718	0.33533
C	-0.00276	0.78019	0.32503
H	0.00306	0.79561	0.37430
C	0.19146	-0.00553	0.21517
P	0.13799	-0.03768	0.16284
C	0.71275	-0.02225	0.69059
P	0.65795	-0.05193	0.63814
O	0.93539	0.95050	0.05738
O	0.84752	0.64845	0.61371
O	0.63680	0.85724	0.37408
O	0.05986	0.05986	0.05986

Table S5. Atomic fractional coordinates of simulated NU-411 in an asymmetric unit

Atom	x	y	z
C	0.8416	0.9754	0.6629
C	0.9950	0.7332	0.2260
C	0.9940	0.6845	0.2400
C	0.0040	0.6485	0.2060
C	0.0155	0.6612	0.1581
C	0.0170	0.7098	0.1445
C	0.0060	0.7458	0.1784
C	0.0100	0.8483	0.3010
C	0.0160	0.8140	0.2650
C	0.9870	0.7728	0.2641
C	0.9520	0.7661	0.3000
C	0.9460	0.8005	0.3360
Zr	0.4090	0.0000	0.0000
O	0.4569	0.9569	0.9569
O	0.3670	0.0000	0.0692
O	0.8670	0.0000	0.5692
O	0.0000	0.3670	0.9308
O	0.0000	0.8670	0.4308
P	0.3846	0.9694	0.1154
P	0.6154	0.0306	0.1154
H	0.1161	0.7994	0.4690
H	0.1806	0.7358	0.4551
H	0.2678	0.7997	0.5718
H	0.2025	0.8624	0.5858
H	0.3914	0.7171	0.4972
H	0.2799	0.6057	0.4728
H	0.2144	0.6671	0.4940
H	0.3256	0.7792	0.5150
O	0.4149	0.6190	0.6070
O	0.3823	0.5856	0.6104
O	0.4569	0.4569	0.4569

Part III. Sorption Properties

N_2 adsorption isotherms were measured on a Micromeritics ASAP 2420 (Micromeritics, Norcross, GA) instrument at 77 K. Brunauer–Emmett–Teller (BET) surface area was calculated using the N2 sorption data in the region P/P_0 = 0.03~0.2. Pore size distributions curves were obtained via DFT calculations using a carbon slit-pore model with a N_2 kernel. The theoretical pore volume values are calculated by V/ρ = 0.32 cm^3/g, where V and ρ are void rate and theoretical density estimated from single-crystal structure.

Table S6. Sorption properties of DUT-52, NU-406, and NU-407 evaluated from N_2 isotherm at 77 K

MOF	BET Surface Area(m^2/g)	N2 uptake at P/P^0 0.99 (cm^3/g)	Pore volume at P/P^0 0.99 (cm^3/g)	Theoretical pore volume (cm^3/g)
DUT-52	1310	361	0.559	0.562
NU-406	1190	321	0.497	0.583
NU-407	445	146	0.226	0.439

H_2O and NH_3 adsorption isotherms were measured on a Micromeritics 3-Flex instrument (Micromeritics, Norcross, GA) instrument at 298 K with a temperature controller. Samples were preactivated with the corresponding methods mentioned in the material preparation section.

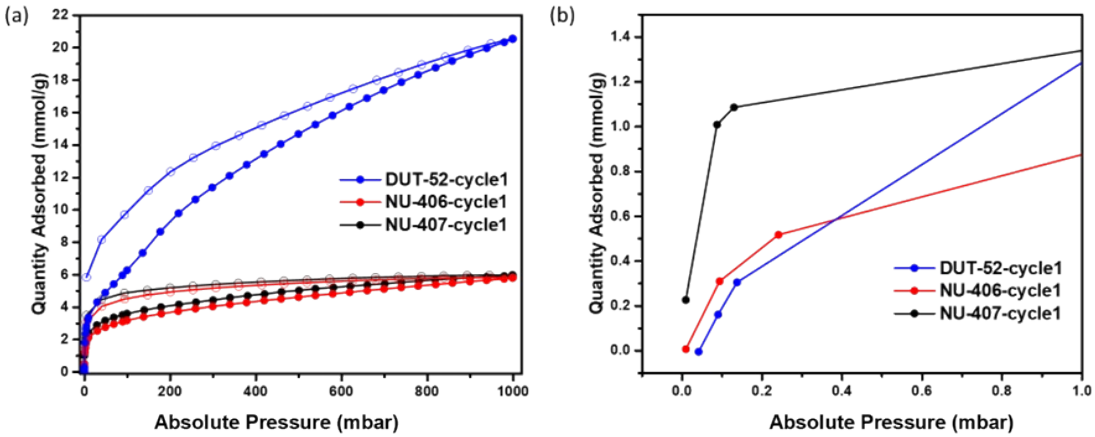

Figure S16. The first cycle of NH_3 adsorption isotherms of DUT-52, NU-406 and NU-407 at 298 K (a) from 0 to 1 bar and (b) the zoom-in to 0-1 mbar.

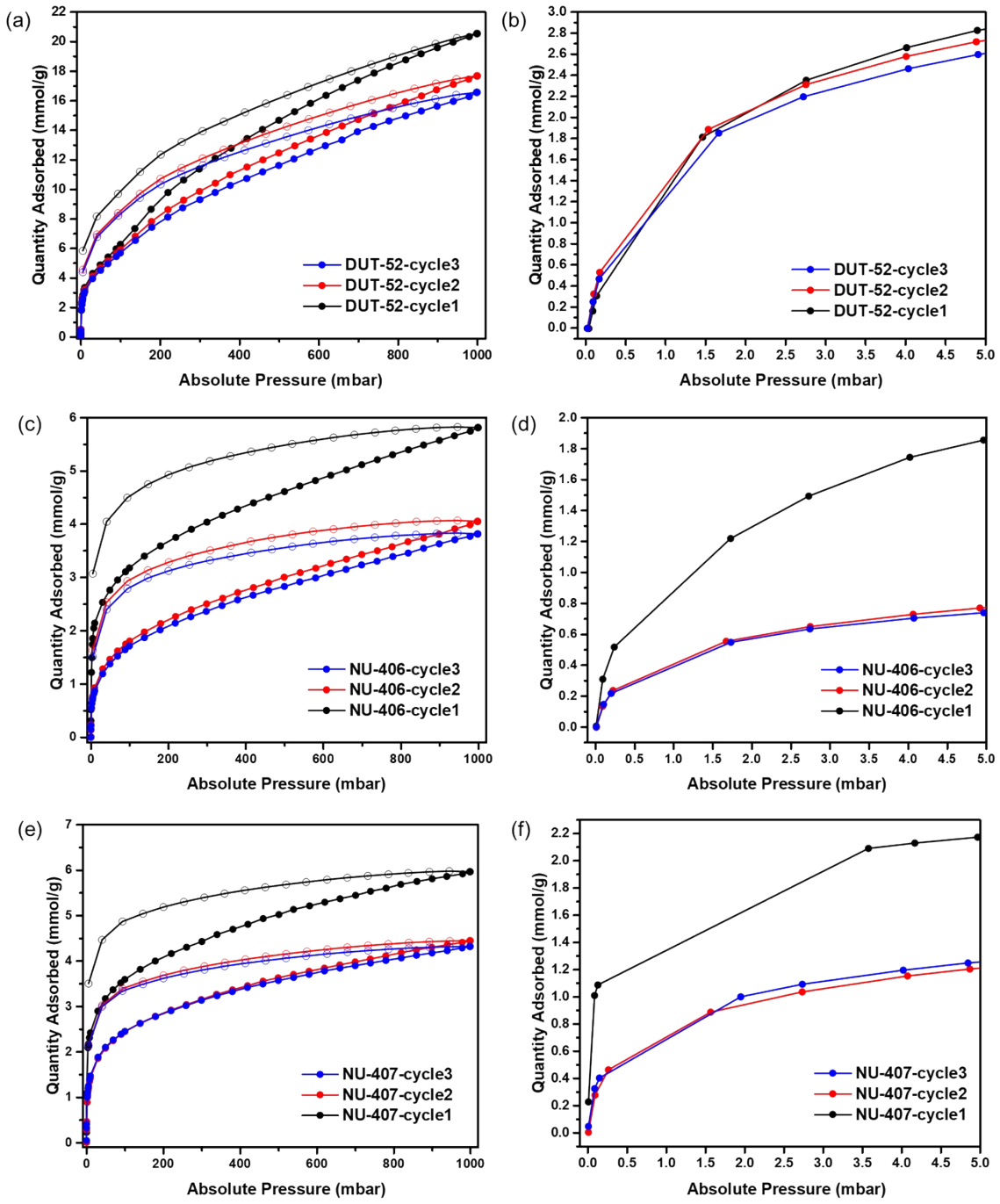

Figure S17. The three cycles of NH_3 adsorption isotherms at 298 K (a), (c), (e) from 0 to 1 bar and the zoom-in (b), (d), (f) to 0-5 mbar of DUT-52, NU-406 and NU-407 respectively.

It is important to note that, although DUT-52 and NU-406 exhibit similar pore volumes, they demonstrate different total uptakes for NH_3 and H_2O. This discrepancy may stem from structural relaxation during the NH_3 and H_2O isotherm measurements. Unlike N_2, which serves as a neutral porosity probe, molecules like NH_3 and water can form strong interactions with the framework, likely through hydrogen bonding. Such interactions might alter the total pore volume available for NH_3 absorption. As highlighted in the manuscript, the framework's phosphorus is sp^3 hybridized, offering more flexibility compared to the more rigid sp^2 hybridized carbon. This flexibility is evidenced by the comparable NH_3 and water uptake in both NU-406 and NU-407.

Part IV. Supplementary Figures

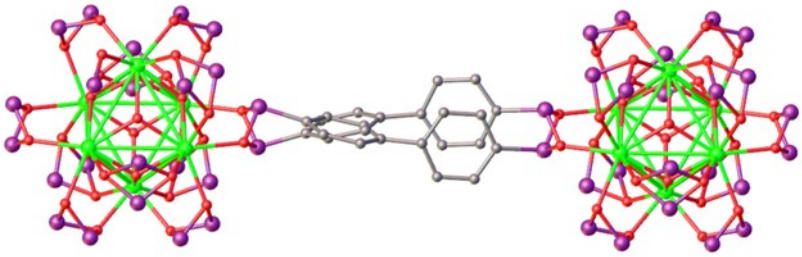

Figure S18. Coordination mode of phosphinate group in NU-410

Scanning electron micrographs (SEM) images were taken using a Hitachi S4800 at the EPIC facility (NUANCE Center-Northwestern University). Samples were dispersed on carbon tapes on an aluminum stub and coated with Os metal to ~9 nm thickness in a Denton Desk III TSC Sputter Coater before imaging.

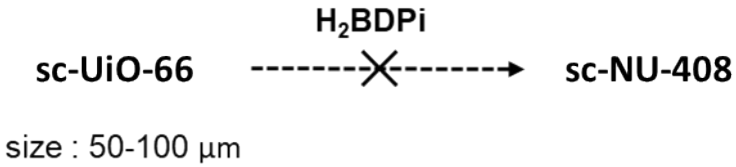

Scheme S1. Attempt of synthesizing single crystal NU-408 via SALE with UiO-66 single crystals as starting materials.

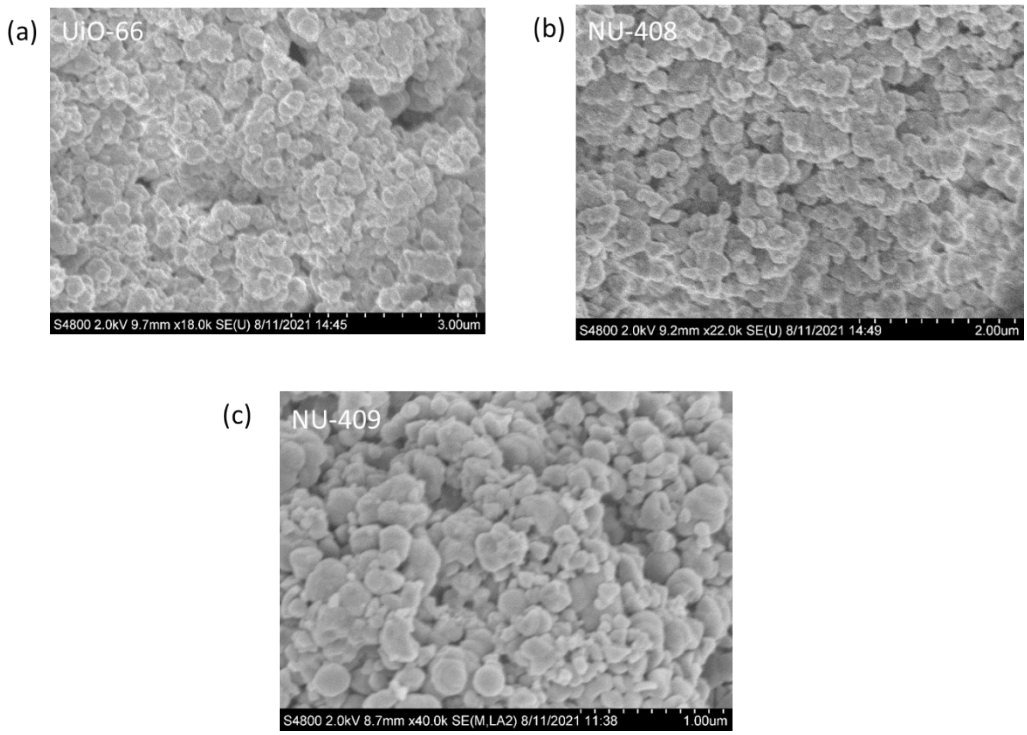

Figure S19. SEM images of (a) UiO-66, (b) NU-408 and (c) NU-409 samples with particle size around 300 nm.

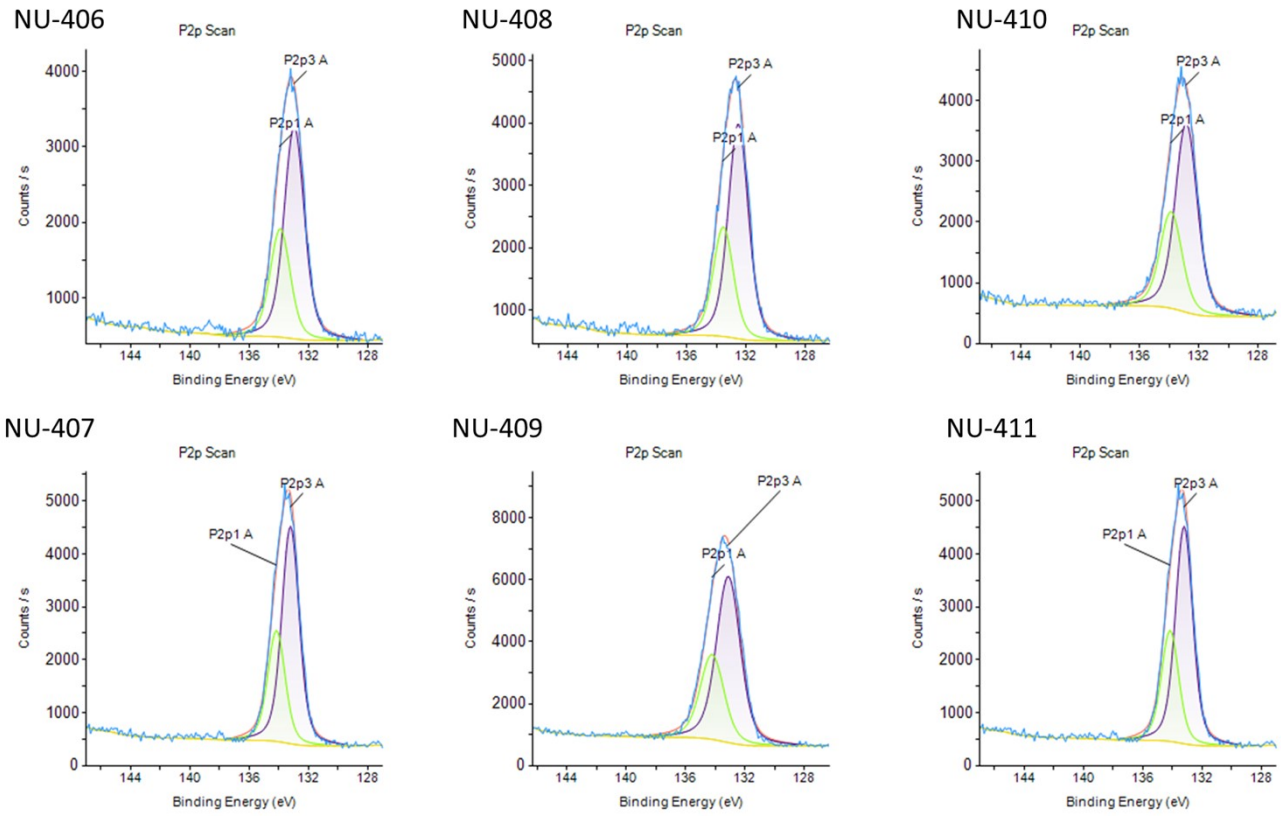

Figure S20. Phosphorus XPS spectra of NU-406, NU-407, NU-408, NU-409, NU-410, NU-411

Table S7. P bonding energy and Zr:P ratio from XPS

MOF	Binding Energy ($P2p_{3/2}$, eV)	Zr:P
NU-406	132.96	0.46
NU-407	133.19	0.59
NU-408	132.55	0.55
NU-409	133.12	0.47
NU-410	132.86	0.48
NU-411	133.21	0.42

The phosphorus bonding energies in phosphinate MOFs are approximately 132.7 eV, while those in phosphonate MOFs are around 133.2 eV. This aligns well with the oxidation of the phosphinate group to the phosphonate group via post-synthetic modifications. Additionally, the Zr:P ratios in both types of MOFs are consistently around 0.5, which corresponds well with the theoretical Zr:P value of 6:12 per Zr_6 node.

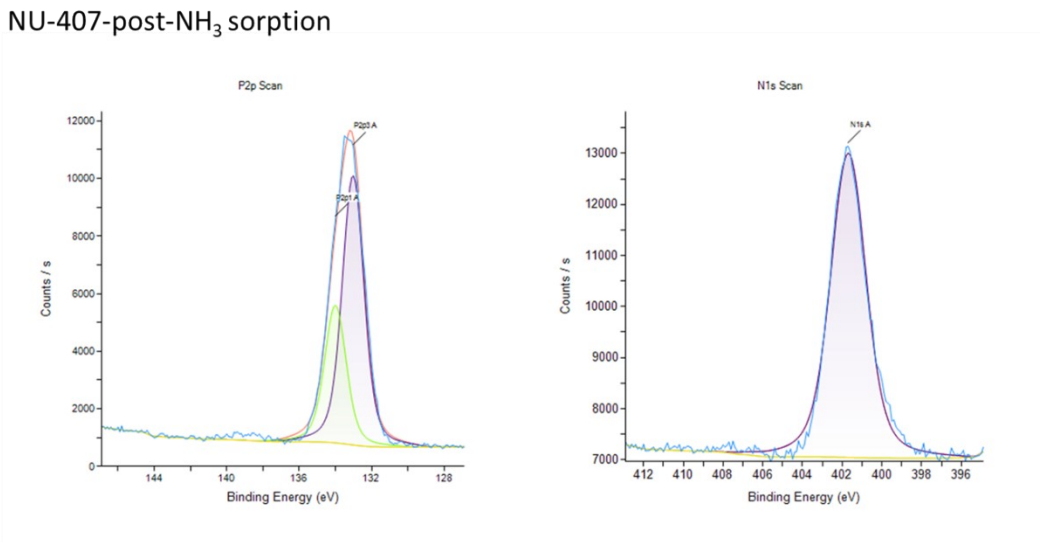

Figure S21. Phosphor and Nitrogen XPS spectra of NU-407 after the NH_3 sorption measurements. The sample was reactivated by dynamic vacuum at room temperature for 24 hours.

Table S8. Bonding energy and N:P ratio from XPS analysis of of NU-407 after NH_3 sorption measurements

MOF	Binding Energy ($P2p_{3/2}$, eV)	Binding Energy (N1s, eV)	N:P
NU-407	133.03	401.69	0.56

XPS measurements of NU-407 after the NH_3 sorption measurements(reactivated under dynamic vacuum at room temperature) were perfomed. A peak for N1s was found at 401.69 eV on the XPS spectra, which corresponds well to the peak position for NH^{4+} in the data base.[3]

Part V. References

1. M. J. Katz, Z. J. Brown, Y. J. Colón, P. W. Siu, K. A. Scheidt, R. Q. Snurr, J. T. Hupp and O. K. Farha, *Chemical Communications*, 2013, **49**, 9449-9451.
2. V. Bon, I. Senkovska, M. S. Weiss and S. Kaskel, *CrystEngComm*, 2013, **15**, 9572-9577.
3. NIST X-ray Photoelectron Spectroscopy Database, NIST Standard Reference Database Number 20, National Institute of Standards and Technology, Gaithersburg MD, 20899 (2000), **DOI:** https://dx.doi.org/10.18434/T4T88K, (retrieved [2024]).